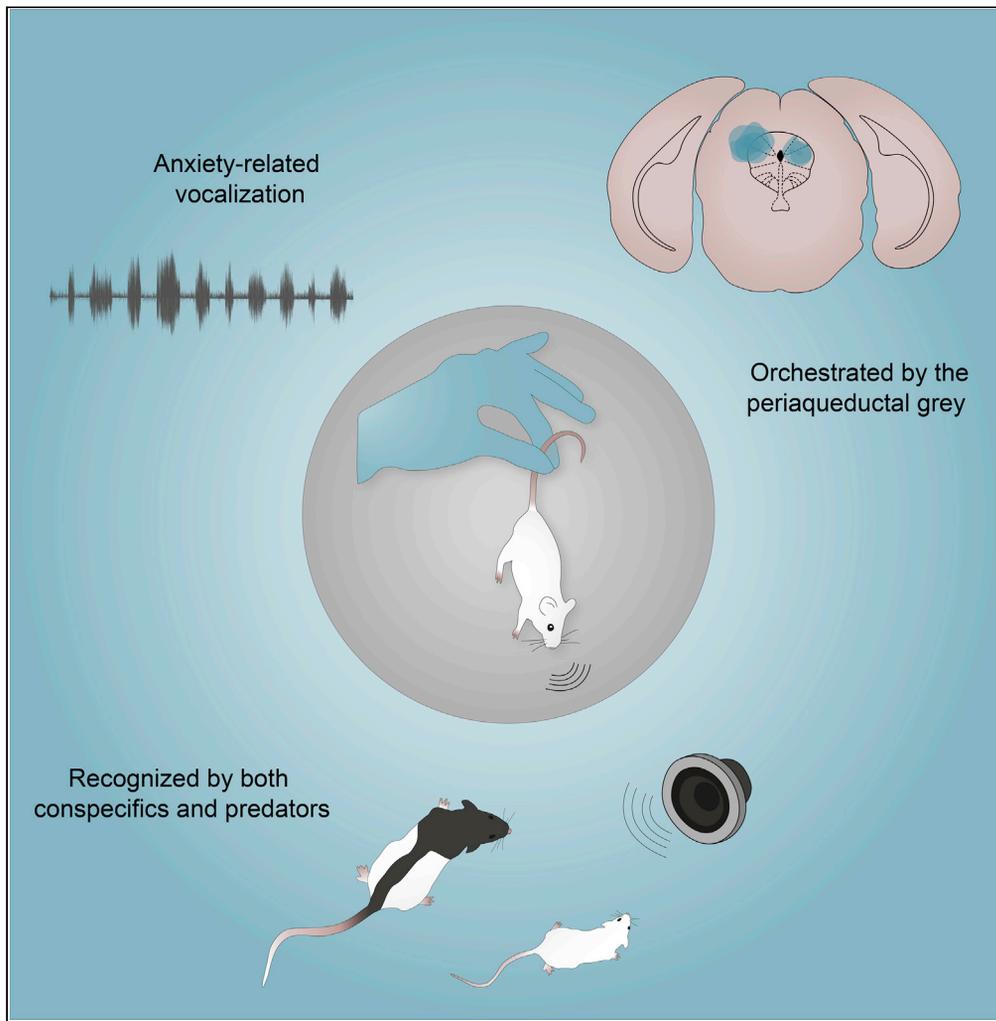## Article

Why do mice squeak? Toward a better understanding of defensive vocalization

Julia Ruat,
Andreas J.
Genewsky, Daniel
E. Heinz, ...,
Michael Czisch,
Alon Chen,
Carsten T. Wotjak

carsten.wotjak@
boehringer-ingelheim.com

Highlights

Sonic vocalization in
threatening situations is
prominent in highly
anxious mice

It coincides with increased
neuronal activity within
the periaqueductal gray
(PAG)

Pharmacological
inhibition of the PAG
attenuates sonic
vocalization

Sonic calls attract both
rats and mice in the
presence of a stimulus
mouse

iScience

Article

Why do mice squeak? Toward a better understanding of defensive vocalization

Julia Ruat,[1,2,3] Andreas J. Genewsky,[2] Daniel E. Heinz,[2,4] Sebastian F. Kaltwasser,[2] Newton S. Canteras,[5] Michael Czisch,[6] Alon Chen,[1,7] and Carsten T. Wotjak[2,8,9,*]

SUMMARY

Although mice mostly communicate in the ultrasonic range, they also emit audible calls. We demonstrate that mice selectively bred for high anxiety-related behavior (HAB) have a high disposition for emitting sonic calls when caught by the tail. The vocalization was unrelated to pain but sensitive to anxiolytics. As revealed by manganese-enhanced MRI, HAB mice displayed an increased tonic activity of the periaqueductal gray (PAG). Selective inhibition of the dorsolateral PAG not only reduced anxiety-like behavior but also completely abolished sonic vocalization. Calls were emitted at a fundamental frequency of 3.8 kHz, which falls into the hearing range of numerous predators. Indeed, playback of sonic vocalization attracted rats if associated with a stimulus mouse. If played back to HAB mice, sonic calls were repellent in the absence of a conspecific but attractive in their presence. Our data demonstrate that sonic vocalization attracts both predators and conspecifics depending on the context.

INTRODUCTION

Vocalization is an essential means of communication that conveys information to conspecifics and across species. It is produced in a diverse range of contexts and emotional states, such as during social interactions like courtship, play, and maternal care, but also in threatening situations in the shape of alarm calls and cries, as well as in response to painful encounters (Blumstein, 2007; Knutson et al., 1999; Lingle et al., 2012; Shen et al., 2008; Whitney et al., 1974; Zippelius and Schleidt, 1956). Vocalization requires an interplay of respiratory, laryngeal, and supralaryngeal components, which are mostly coordinated via hindbrain nuclei (Fitch, 2006; Hernandez-Miranda et al., 2017; Holstege and Subramanian, 2016; Jürgens, 2009; Wetzel et al., 1980). Decades of work established that the midbrain periaqueductal gray (PAG) is a crucial gating center for vocalization in many species, from fish to humans (Fenzl and Schuller, 2002; Green et al., 2018; Jürgens, 2009; Kittelberger et al., 2006; Tschida et al., 2019). For instance, bilateral lesions or traumatic injury of the PAG lead to mutism, whereas electrical or neurochemical stimulation triggers natural vocalization sounds (Adametz and O'Leary, 1959; Esposito et al., 1999; Jürgens, 1994; Kyuhou and Gemba, 1998; Magoun et al., 1937; Shipley et al., 1991; Skultety, 1962; Zhang et al., 1994). In mice, recent work has discovered a specific subpopulation of PAG neurons and their hypothalamic inputs that mediate vocalization (Chen et al., 2021; Gao et al., 2019; Michael et al., 2020; Tschida et al., 2019). Research on mouse vocalization has mainly focused on ultrasonic vocalization (USV). However, additional to these sounds that are inaudible for humans, mice also emit squeaks and squeals that are well within the human hearing range. Compared to our growing understanding of mouse USV neuronal circuits, as well as its functions (Fischer and Hammerschmidt, 2011; Holy and Guo, 2005; Lahvis et al., 2011; Portfors, 2007; Sangiamo et al., 2020) and its implications in mouse models of psychiatric disorders like autism, schizophrenia, and mania (Malkesman et al., 2009; Scattoni et al., 2009, 2011; Scearce-Levie et al., 2008; Wöhr and Schwarting, 2013), sonic vocalization has received by far less attention. Early reports refer to observations of singing house mice (Coburn, 1912; Dice, 1932) and describe sonic squeaks in the context of pain cries (Ehret, 1974; Scott, 1946) and defensive behaviors (Blanchard et al., 1998; Gourbal et al., 2004; Houseknecht, 1968; Yang et al., 2006). Yet, the characteristics of sonic mouse vocalization and the underlying neuronal circuits and ecological relevance are largely unexplored.

In the current study, we used a mouse line that was selectively bred for high anxiety-related behavior (HAB, Krömer et al., 2005) in which we had observed a high disposition of sonic calls during handling. We studied (i) the characteristics of the sonic calls in comparison to other mouse lines, (ii) assessed the consequences of

[1]Department Stress Neurobiology and Neurogenetics, Max Planck Institute of Psychiatry, 80804 Munich, Germany

[2]Research Group Neuronal Plasticity, Max Planck Institute of Psychiatry, 80804 Munich, Germany

[3]International Max Planck Research School for Translational Psychiatry (IMPRS-TP), 80804 Munich, Germany

[4]Max Planck School of Cognition, Max Planck Institute for Human Cognitive and Brain Sciences, 04303 Leipzig, Germany

[5]Department of Anatomy, Institute of Biomedical Sciences, University of São Paulo, São Paulo 05508-000, Brazil

[6]Scientific Core Unit Neuroimaging, Max Planck Institute of Psychiatry, 80804 Munich, Germany

[7]Department of Neurobiology, Weizmann Institute of Science, Rehovot 76100, Israel

[8]Present address: Central Nervous System Diseases Research (CNSDR), Boehringer Ingelheim Pharma GmbH & Co KG, 88397 Biberach an der Riss, Germany

[9]Lead contact

*Correspondence: carsten.wotjak@boehringer-ingelheim.com

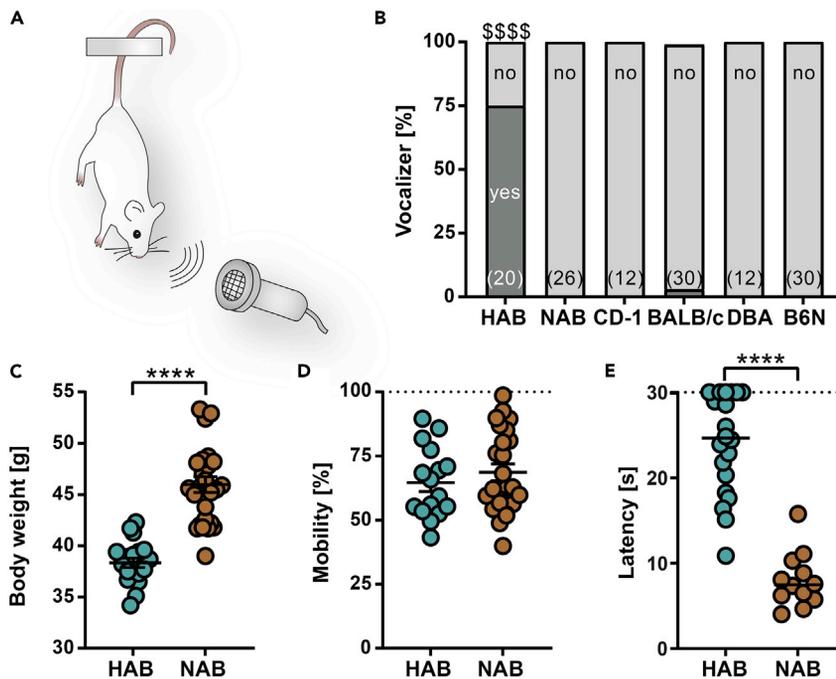https://doi.org/10.1016/j.isci.2022.104657

Figure 1. Mice bred for high anxiety-related behavior have a higher disposition for sonic vocalization

(A) Sonic calls were triggered during a 5-min tail suspension and recorded using an ultrasound microphone.

(B) Percentage of male mice of various mouse lines emitting sonic calls during tail suspension. HAB, high anxiety-related behavior; NAB, normal anxiety-related behavior; B6N: C57Bl/6. Numbers in parenthesis indicate group sizes.

(C) Body weight of HAB (n = 20) and NAB (n = 26) mice.

(D) Mobility behavior during the tail suspension.

(E) Latency to hind paw flicks or licking during a hot plate test (n = 20 HAB, n = 12 NAB).

Data are presented as a percentage of total (B), individual data with mean $\pm$ SEM (C and D), and median

(E). $^{\$\$\$\$}p < 0.0001$ (Chi square test), $^{****}p < 0.0001$ (unpaired t test).

anxiolytic versus panicolytic compounds, (iii) dissected the neuronal circuits for sonic vocalization by means of manganese-enhanced magnetic resonance imaging (MEMRI, Almeida-Corrêa et al., 2018; Bedenk et al., 2018), tracing, as well as pharmacological and chemogenetic methods and (iv) investigated the ecological function of sonic calls in regard to conspecifics and predators.

RESULTS

Mice bred for high anxiety-related behavior have a high disposition for sonic vocalization

Based on our observation that HAB mice emit sonic calls when lifted by their tail, we used the classic tail suspension test (TST) to trigger and record sonic vocalization (Figure 1A). To investigate whether this vocalization behavior is specific to HAB mice, we tail suspended normal anxiety-related behavior (NAB, originating from the same CD-1 strain by selective breeding), CD-1, BALB/c, DBA, and C57BL/6 (B6N) mice and quantified the vocalization events compared to HAB animals. During a 5-min TST, 75% of HAB mice emitted sonic calls, whereas neither NAB, CD-1, nor B6N and only one out of 30 BALB/c mice produced sonic vocalization ($\chi^2 = 86.3$, $p < 0.0001$; Figure 1B). In addition, female HAB mice produced sonic vocalization when suspended by the tail, although at a lower percentage than males (26%; $\chi^2 = 9.2$, $p < 0.01$, data not shown, same male HAB cohort as depicted in Figure 1B). Although the increased body weight of NAB compared to HAB mice ($t_{44} = 7.9$, $p < 0.0001$; Figure 1C) suggests greater tissue stress, in fact the struggling behavior did not differ between the two strains ($t_{38} = 0.8$, $p = 0.41$; Figure 1D). In the hotplate test, HAB mice showed even a significantly lower pain sensitivity than NAB mice ($U = 3$, $p < 0.0001$; Figure 1E). These findings exclude increased levels of physical stress and pain as the driving forces behind the elevated susceptibility of HAB mice for sonic vocalization.

Male HAB mice did not vocalize more in general, as fewer animals emitted ultrasonic calls compared to male NAB mice in the presence of a female conspecific ($\chi^2 = 4.1$, $p < 0.05$; Figure 2A), which was also
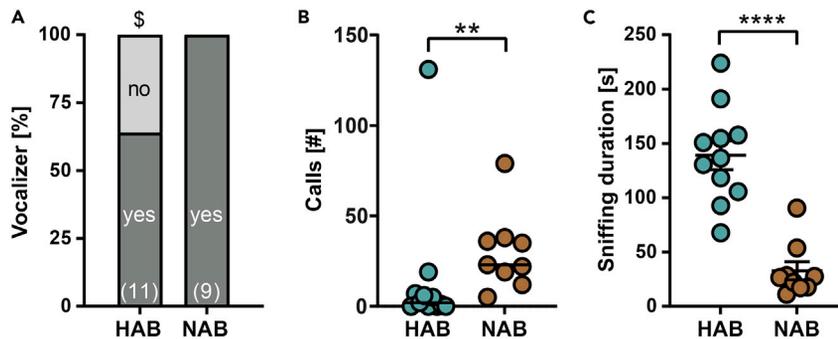
Figure 2. Mice bred for high anxiety-related behavior produce less female-induced ultrasonic vocalization

(A) Percentage of male high anxiety-related behavior (HAB; n = 11) and normal anxiety-related behavior (NAB; n = 9) mice emitting ultrasonic calls in the presence of a same-strain female.

(B) Number of ultrasonic calls emitted during 10 min of interaction (not corrected for outliers).

(C) Total duration of anogenital and facial sniffing by male mouse.

Data are presented as a percentage of total (A), individual data with median (B), and mean ± SEM (C). $^{\$}$p < 0.05 (Chi square test), **p < 0.01 (Mann-Whitney test), ****p < 0.0001 (unpaired t test).

reflected by a lower number of female-induced USVs (U = 14, p < 0.01; Figure 2B). The reduced USV was unrelated to the social investigation behavior, which was even more pronounced in HAB mice (t_{18} = 6.4, p < 0.0001; Figure 2C). Thus, the lower prevalence of USV shown by HAB mice does not relate to any deficits in male-female social interaction.

Sonic vocalization is sensitive to anxiolytics

To gain insight into potential systems involved in the regulation of sonic vocalization, we treated mice systemically with anxiolytic and panicolytic compounds before the TST. Diazepam-treated HAB mice showed a trend to a reduction in the number of vocalizing animals compared to vehicle-treated HAB mice (χ^2 = 3.55, p = 0.06; Figure 3A), with the number of emitted sonic calls significantly decreased (U = 31.5, p < 0.05; Figure 3B). Mobility during the TST, in contrast, was unaffected (U = 57, p = 0.57; Figure 3C). Further, diazepam treatment of male mice before a social interaction with a female did not alter the number of USVs emitted compared to vehicle-treated controls (U = 59.5, p = 0.69; data not shown). This demonstrates the sensitivity of sonic, but not USV to anxiolytic drugs.

Given the panicolytic effects of activated anandamide signaling (Heinz et al., 2017), we blocked the main degrading enzyme of this endocannabinoid, fatty acid amide hydrolase (FAAH), before the TST. Neither of the doses of the FAAH inhibitor URB597 (0.3 nor 1 mg/kg) influenced the proportion of animals vocalizing (χ^2 = 0.72, p = 0.70; Figure 3D), the number of calls emitted ($F_{2,36}$ = 0.06, p = 0.94; Figure 3E), nor the mobility ($F_{2,35}$ = 1.24, p = 0.30; Figure 3F). To rule out that anandamide signaling had already been sufficiently activated by the test procedure, which would have occluded any further changes by URB597 treatment, we administered the cannabinoid receptor type 1 (CB1) antagonist/inverse agonist SR141716A to a new cohort of mice prior to the TST. Again, we did not observe any changes in the proportion of vocalizing animals (χ^2 = 0.02, p = 0.88; Figure 3G), the number of calls (t_{17} = 0.66, p = 0.52; Figure 3H), or the struggling behavior during the TST (U = 36, p = 0.44; Figure 3I). Taken together, we could show that sonic vocalization is sensitive to anxiolytics but found no evidence for endocannabinoid involvement.

The dorsolateral periaqueductal gray controls sonic vocalization

In a next step, we aimed at dissecting the central pathways controlling the high levels of anxiety and sonic vocalization in HAB mice. To identify candidate brain regions, we assessed the accumulation of manganese as a measure for tonic neuronal activity using repeated manganese (MnCl$_2$) treatment of naïve mice followed by MEMRI. We identified several brain regions with differences in manganese accumulation when comparing male HAB and NAB mice (Figure 4A). Among others, HAB mice seem to have a decreased tonic neuronal activity of the superior colliculus and the reticular nucleus. Conversely, manganese accumulation was increased in the lateral septum, the hippocampus, the interpeduncular nucleus, and the rostral and caudal PAG (Figures 4B and 4C, see Figure S1).
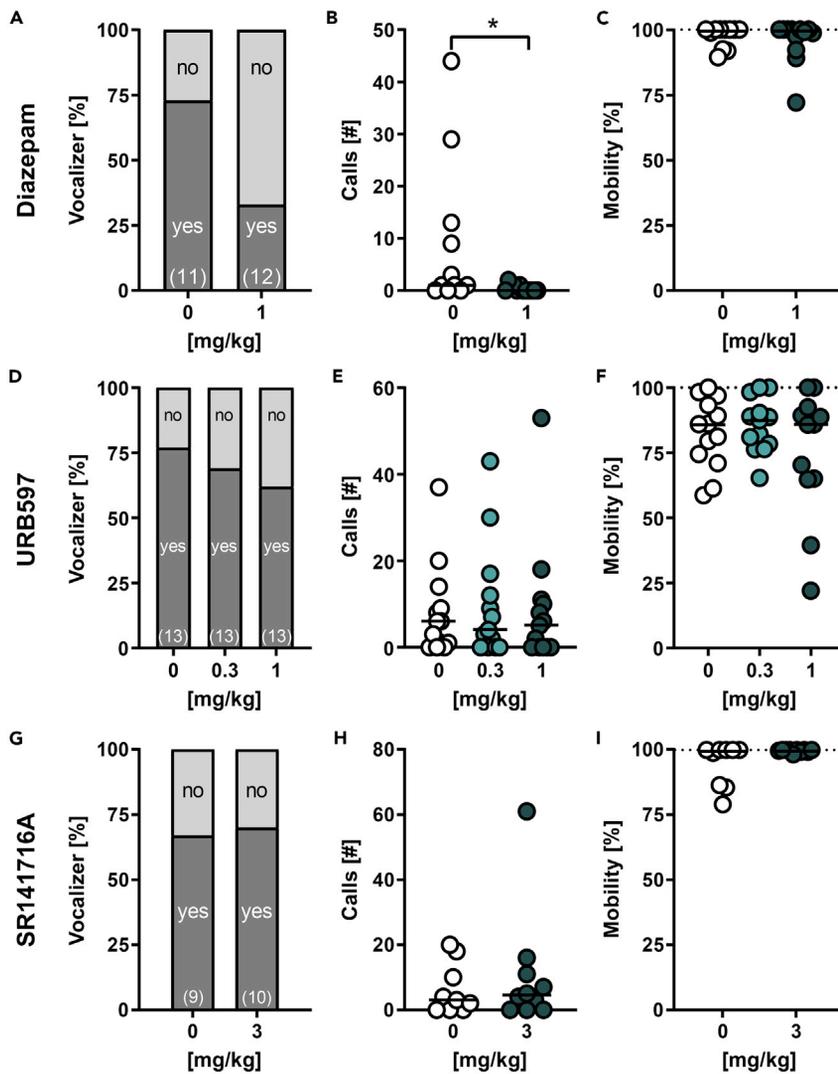
Figure 3. Sonic vocalization is sensitive to anxiolytics

Percentage of high anxiety-related behavior (HAB) mice emitting sonic calls (A, D, and G), number of calls emitted per mouse (B, E, and H), and mobility behavior (C, F, and I) during tail suspension (2.5 min) 60 min after systemic administration of diazepam (A–C), FAAH inhibitor URB597 (D–F), or CB1 receptor antagonist/inverse agonist SR141716A (G–I). Data are presented as percentage of total (A, D, G) and individual data with median (B and C, E and F, H and I). *p < 0.05 (Mann Whitney test). Animal numbers per treatment group are indicated in parentheses in the figures.

To test whether the tonic increase in neuronal activity of the dorsolateral PAG (dlPAG) revealed by MEMRI translates into increased vocalization and anxiety-related behavior, we locally infused muscimol (MUSC) into the dlPAG of a new cohort of HAB mice before TST and exposure to the elevated plus-maze (EPM). An exemplary image of MUSC diffusion is depicted in Figure 4E. The diffusion comprised the dlPAG and the lateral PAG and partly the deep and intermediate layers of the superior colliculus (see Figure S2). MUSC application before the TST (Figure 4D) completely abolished sonic vocalization (χ^2 = 20.1, p < 0.0001, Figure 4F; U = 14, p < 0.0001, Figure 4G). In contrast, mobility was significantly increased (U = 39, p < 0.05; Figure 4H). Importantly, the same intervention caused the animals to spend significantly less time in the closed (t_9 = 3.7, p < 0.01; data not shown) and significantly more time in the open arms of an EPM compared to vehicle-treated controls (U = 1, p < 0.01, Figure 4I). This finding further supports the close link between increased anxiety-related behavior and high levels of sonic vocalization and suggests an essential role for the PAG in this interaction.

Because the intraneuronal accumulation of manganese is biased toward axon terminals (Bedenk et al., 2018), we aimed to identify brain areas projecting to the PAG. We injected the retrograde tracer Fluoro-Gold (FG)
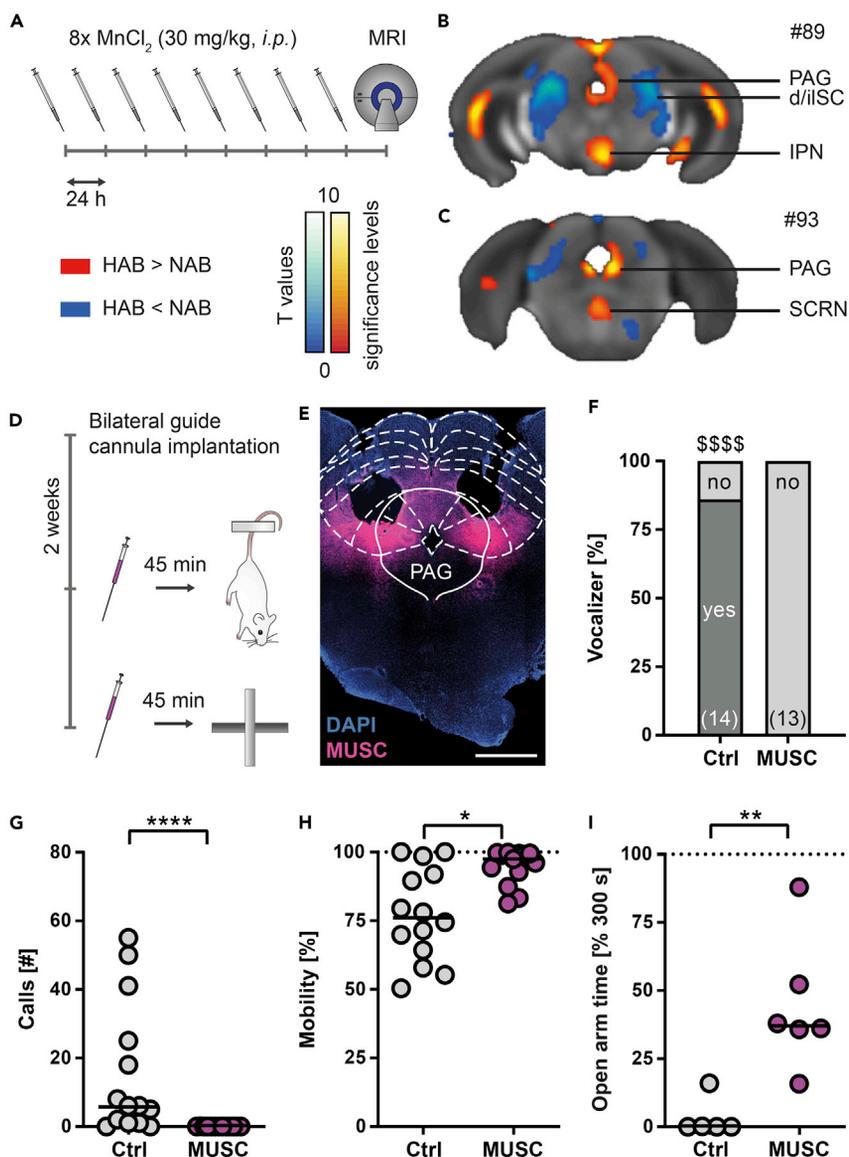
Figure 4. The dorsolateral periaqueductal gray controls sonic vocalization

(A–C) Manganese-enhanced magnetic resonance imaging (MEMRI) comparing high anxiety-related behavior (HAB) vs. normal anxiety-related behavior (NAB) mice. (A) HAB (n = 31) and NAB (n = 26) mice received daily systemic manganese injections (8 days, 30 mg/kg per day) and underwent MRI scanning 24 h after the last injection.

(B–C) Increased tonic neuronal activity in the caudal periaqueductal gray (PAG) of HAB mice. Statistical threshold is set at $p < 0.0001$, cluster extent >50. d/ilSC, deep/intermediate layers of superior colliculus; IPN, interpeduncular nucleus; SCRN, superior central raphe nucleus. Numbers (#) indicate image numbers of corresponding reference images in the Allen Brain Atlas. See also Figure S1.

(D–I) Local inhibition of the dlPAG using muscimol (MUSC).

(D) MUSC was bilaterally injected via guide cannulas into the dlPAG 45 min before the TST and EMP (n = 14).

(E) Representative image of the injection site. Scale bar: 1 mm. See also Figure S2. (F) Percentage of HAB mice emitting sonic calls, (G) the number of calls emitted per mouse, and (H) mobility behavior during the tail suspension (5 min).

(I) Open arm time on the Elevated Plus Maze (EPM) during the first 5 min of the test.

Data are presented as percentage of total (F) or individual data with median (G–I). $^{\$\$\$\$}p < 0.0001$ (Chi square test), $^*p < 0.05$, $^{**}p < 0.01$, $^{****}p < 0.0001$ (Mann-Whitney test).

unilaterally into the dlPAG of HAB mice (see Figure S3A) and found FG-labeled cells in the medial prefrontal cortex (mPFC), more specifically the infralimbic, prelimbic, and cingulate cortex, and the secondary motor area (see Figures S3B and S3C). Less dense labeling was observed in the lateral septum (see Figure S3D). FG-positive cells
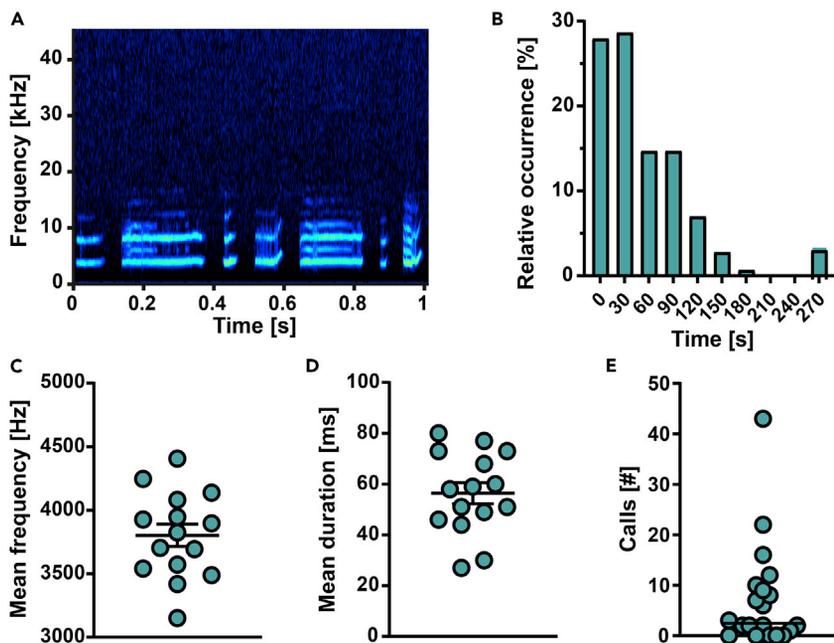
Figure 5. Mice bred for high anxiety-related behavior emit sonic calls when caught by the tail

(A) Representative spectrogram displaying various high anxiety-related behavior (HAB) calls.

(B) Relative frequency of calls emitted by HAB mice (n = 20) over the course of a 5-min tail suspension.

(C) Mean fundamental frequency of HAB calls.

(D) Mean duration of HAB calls per animal.

(E) Number of calls emitted per mouse during tail suspension.

Data are presented as relative occurrence (B), individual data with mean ± SEM (C and D), or median (E).

could also be seen in the medial and lateral preoptic area and the bed nucleus of stria terminalis (see Figure S3E). Strong labeling was shown in the ventromedial hypothalamus and the zona incerta, and a few FG-positive cells could be observed in the dorsomedial hypothalamus (see Figure S3F). Given the evidence for a strong projection from mPFC to the dlPAG and earlier reports on the role of the mPFC in controlling vocalization in rats, monkeys, and humans (Bennett et al., 2019; Jürgens and von Cramon, 1982; Sutton et al., 1974), we employed a double-viral approach to chemogenetically inhibit the pathway (see Figures S3G and S3H). The intervention neither affected the number of vocalizing animals ($\chi 2$ = 0.1, p = 0.75; see Figure S3I) nor the number of calls emitted (U = 65, p = 0.49; see Figure S3J), nor the struggling behavior (U = 56.5, p = 0.38; see Figure S3K) during the TST. Conversely, the inhibition of the mPFC-dlPAG pathway led to a decrease in avoidance behavior upon confrontation with an erratically moving robo-beetle ($t23$ = 2.4, p < 0.05; see Figure S3L), thus demonstrating the sufficiency of the approach to interfere with innate fear. Consequently, other projections to the PAG but from the mPFC seem to mediate sonic vocalizations in HAB mice.

Sonic mouse calls are appetitive to rats and mice in the presence of a social stimulus

Because vocalization aims at transmitting information to other individuals, we wanted to clarify the ecological function of sonic HAB calls. In the first step, we analyzed the characteristics of the calls. A representative spectrogram of sonic calls of HAB mice is depicted in Figure 5A. The recorded calls follow a harmonic structure with a flat pattern showing very little modulation in frequency. Furthermore, nonlinear features such as subharmonics and deterministic chaos (for review on nonlinearities see Fitch et al., 2002) can be detected in the spectrogram of the calls (Figure 5A). Most calls were emitted during the first minute of the TST and vocalization declined over time (Figure 5B). Analysis of the characteristics of the calls emitted by male HAB mice revealed a mean fundamental frequency of 3,802 ± 87.6 Hz (Figure 5C) with a mean duration of 56.4 ± 4.2 ms (Figure 5D). During a 5-min TST, male HAB mice emitted a variable number of calls, with a median call number of 7 calls (Figure 5E). To compare the measured fundamental frequency of TST-triggered calls with those emitted in other behavioral test situations and by other strains, we subjected male HAB and B6N mice to a social defeat paradigm. Sonic calls emitted by defeated HAB mice were comparable in terms of fundamental
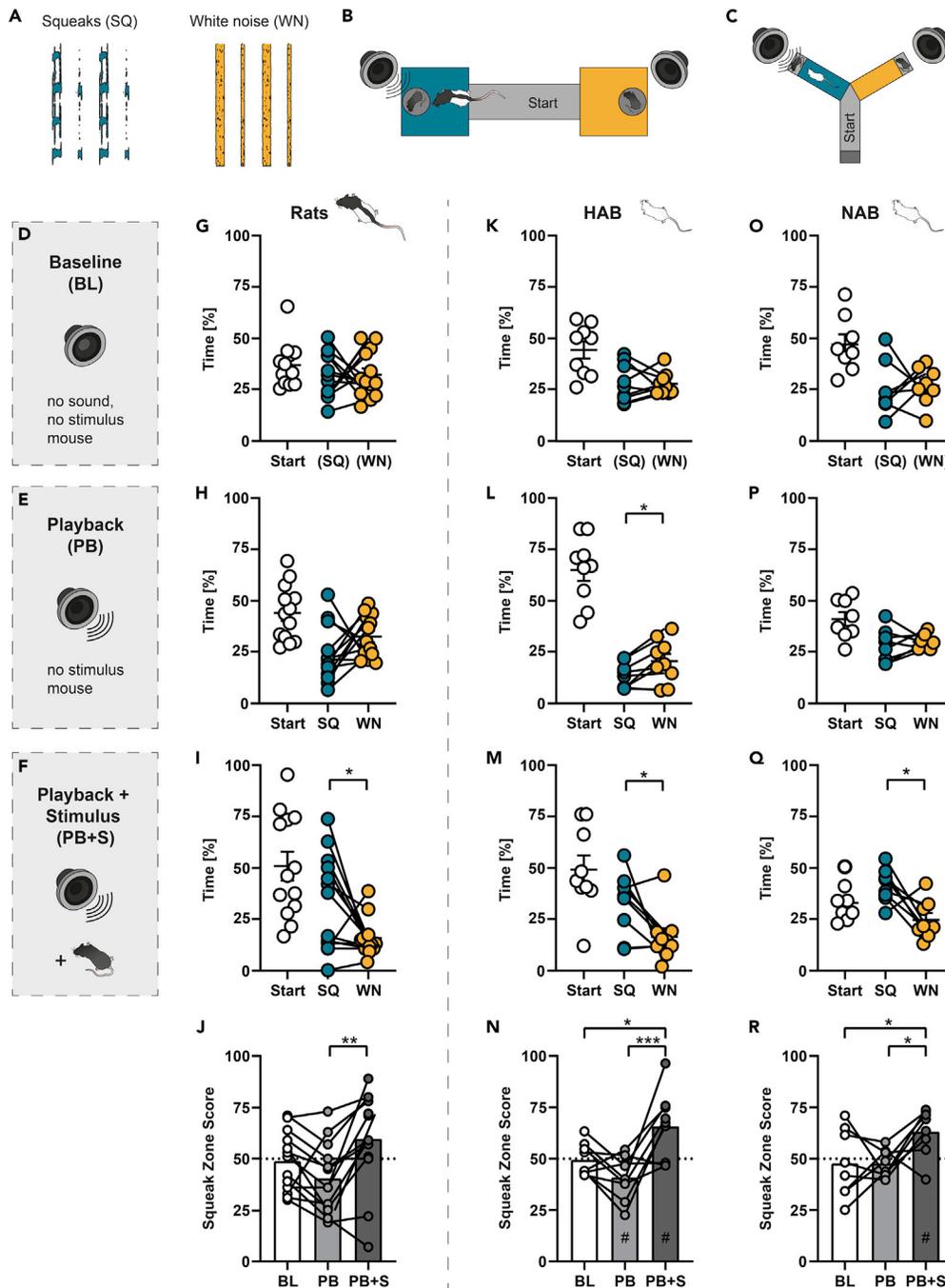
Figure 6. Sonic mouse calls are appetitive to rats and mice in the presence of a social stimulus

(A) High anxiety-related behavior (HAB) squeaks (SQ) or control time- and amplitude-matched white noise (WN) served as stimulus sounds (depicted here schematically). See also Figure S5.

(B) Setup for rat (n = 13) playback experiment with two playback compartments and a connecting corridor.

(C) Playback experiment with HAB (n = 9) and normal anxiety-related behavior (NAB; n = 8) mice were performed in a Y-maze with two playback compartments and a start arm where no sound was presented.

(D) During the baseline stage (BL), animals could freely explore the maze without sound presentation or stimulus mouse.

(E) Squeaks or white noise were played back once the animal had entered the respective zone during the playback stage (PB) without additional stimulus mouse.

(F) During the last stage (Playback + Stimulus, PB + S), the sounds were presented with an additional male stimulus mouse being present in each playback zone.

Figure 6. Continued

(G–R) Percentage of time spent in each zone is presented for rats (G–I), HAB (K–M), and NAB (O–Q). The squeak zone score for each stage of rats (J), HAB (N), and NAB (R). See also Figure S6.

Data are presented as individual data with mean ± SEM (G–I, K–M, O–Q) or individual data with mean (J, N, and R).

*p < 0.05, **p < 0.01, ***p < 0.001 (paired t test for I, L, M, and Q; RM 1-way ANOVA followed by Tukey's post hoc test for J, N, R), #p < 0.05 (one sample t test for N and R).

frequency to those emitted during a TST (3,872 ± 116 Hz) and those of defeated B6N mice (3,870 ± 192 Hz, Figure S4).

The fundamental frequency of the recorded calls falls within the best hearing frequencies for numerous predators (Heffner and Masterton, 1980; Heffner and Heffner, 1985, 2007; Kelly and Masterton, 1977; Malkemper et al., 2015). Because rats can be muricide in the wild (Blanchard and Caroline Blanchard, 1977; O'Boyle, 1974), we set up a playback experiment where recordings of TST-triggered sonic calls of HAB mice or a white noise control sound (Figure 6A, see Figure S5 and supplemental audio file) were presented to male Long-Evans rats (Figure 6B). The animals could control the presentation of the acoustic stimuli by their own behavior, thus turning it into a kind of real-time place-preference/place-avoidance paradigm. At baseline (BL; no sound presentation, no stimulus mouse; Figure 6D), rats showed no preference for one of the prospective stimulus zones (t_{12} = 0.27, p = 0.80; Figure 6G). Similarly, no preference was observed during the playback (PB) stage during which sonic calls (squeaks) and white noise sounds were presented (t_{12} = 1.62, p = 0.13; Figures 6E and 6H). In the third stage of the test, male B6N stimulus mice were constrained to each playback zone in order to make the sound presentation more relevant by presenting a social stimulus (PB + S, Figure 6F). In the presence of stimulus mice, rats showed a preference for the squeak zone (t_{12} = 2.51, p < 0.05; Figure 6I). To illustrate these results more clearly, we calculated the Squeak Zone Score that indicates the preference for the squeak zone with values above 50. Rats showed a significantly higher Squeak Zone Scores in the PB + S compared to the PB stage ($F_{2,24}$ = 6.61, p < 0.01; Figure 6J). Hence, potential predators are attracted to the squeaks if presented together with a real-life prey/ mouse.

Even though the fundamental frequency of the squeaks falls below the best hearing frequencies of mice (Heffner and Masterton, 1980; Heffner and Heffner, 2007), the harmonics at higher frequencies render it likely that sonic calls may serve as alarm signals for conspecifics. Therefore, we repeated the playback experiments with HAB and NAB mice, analogously to the playback experiment with rats (Figure 6C). During the BL period, both HAB (t_8 = 0.12, p = 0.92; Figure 6K) and NAB (t_7 = 0.26, p = 0.80; Figure 6O) mice spent equal amounts of time in the prospective playback arms of the test apparatus. Upon presentation of the sounds in the PB stage, HAB mice spent less time in the squeak zone compared to the white noise zone (t_8 = 3.20, p < 0.05; Figure 6L). This effect was not observed in NAB mice (t_7 = 0.66, p = 0.53; Figure 6P). Despite avoiding the squeak zone during the PB stage, HAB mice spent more time in the squeak zone compared to the white noise zone in presence of a stimulus animal during the PB + S stage (t_8 = 2.70, p < 0.05; Figure 6M). Likewise, NAB mice preferred the squeak zone over the white noise zone during the PB + S stage (t_7 = 3.07, p < 0.05; Figure 6Q). Considering the Squeak Zone Score, HAB mice showed an aversion for the squeak zone when only the sound was presented (t_8 = 2.64, p < 0.05) but preferred this arm once a stimulus animal was present together with the sound (t_8 = 2.85, p < 0.05 and $F_{2,16}$ = 11.47, p < 0.001; Figure 6N, see Figure S6). For NAB mice, the preference is only significant in the presence of a stimulus mouse during PB + S (t_7 = 3.19, p < 0.05 and $F_{2,14}$ = 4.76, p < 0.05; Figure 6R, see Figure S6). Together, these data indicate the aversive nature of squeaks per se to the highly anxious HAB mice. In combination with a social stimulus, however, avoidance turned into approach behavior not only in HAB but also in NAB mice.

DISCUSSION

Mice bred for high anxiety-related behavior (HAB, Krömer et al., 2005) show a high disposition to vocalize when suspended by the tail compared to other mouse lines, which was not explained by different stress coping strategies or higher pain sensitivity. Sonic vocalization was sensitive to anxiolytic but not panicolytic treatment and was dependent on the dorsolateral PAG. Playback of sonic calls to rats and mice revealed that the squeaks trigger approach behavior, however only in the presence of a stimulus mouse.

When suspended by the tail, only HAB mice reliably vocalized. This was not related to a higher body weight, increased struggling during the test or increased pain sensitivity. Conversely, HAB mice emitted less USVs

during interaction with females despite an increase in exploration time. This dissociation stands in contrast to mouse models of autism, whereby the impairment in female-induced USV emission shown by BTBR T + tf/J mice was reported to coincide with reduced investigation times (Scattoni et al., 2011). Yet, an impairment in social behavior has also been found in juvenile HAB rats, which show reduced play behavior accompanied by decreased 50-kHz USV compared to NAB and LAB rats (Lukas and Wöhr, 2015). In terms of anxiety-related vocalization, it has been repeatedly shown that HAB mouse and rats pups emit more isolation-induced USVs than pups of the NAB and LAB lines (Borta et al., 2006; Bosch et al., 2006; Frank et al., 2006; Kessler et al., 2011; Krömer et al., 2005; Wigger et al., 2001).

Audible vocalizations have been reported in the context of predatory defense. Along the predatory imminence continuum (Fanselow and Lester, 1988), anxiety-like and fear behaviors such as risk assessment and freezing decrease with increasing proximity to the predator and switch to explosive, panic-like behaviors such as fighting, biting, jumping, and vocalizations in response to an attack (for review see Perusini and Fanselow, 2015). Increasing anandamide signaling via CB1 receptors has been shown to reduce panic-like behaviors in HAB mice upon confrontation with an erratic moving robo-beetle (Heinz et al., 2017). Therefore, we treated HAB mice with URB597 to inhibit FAAH activity. However, the treatment did not show any effect on sonic vocalizations, neither did treatment with a CB1 receptor antagonist. Together these findings speak against an involvement of endocannabinoid signaling in sonic vocalization. In contrast, treatment with the anxiolytic diazepam significantly reduced the number of sonic calls without affecting female-induced USV. In summary, sonic vocalization seems to be more closely connected to anxiety than panic. Interestingly, HAB mouse pups emit a higher number of isolation-induced USV (Frank et al., 2009; Kessler et al., 2011; Krömer et al., 2005), a behavior associated with anxiety (Fish et al., 2000) that was also reduced by diazepam administration (Krömer et al., 2005).

We employed MEMRI to relate the increased disposition of HAB mice for emitting sonic calls because of increased basal anxiety levels to tonically increased neuronal activity. Manganese enters neurons through ion channels in an activity-dependent manner (Almeida-Corrêa et al., 2018; Bedenk et al., 2018). Owing to its paramagnetic characteristics, manganese can be quantified *in vivo* using MRI. Voxel-wise comparisons of HAB and NAB mice revealed, among others, increased manganese accumulation in the septal-hippocampal complex, which has been suggested as a key circuit implicated in generalized anxiety (Gray and McNaughton, 1996). In addition, we observed increased manganese levels within the PAG. Local muscimol infusion into the PAG completely abolished sonic vocalizations and significantly reduced anxiety-like behavior. The PAG has been established as a gating center for vocalization across many species (Jürgens, 2009), including mice (Chen et al., 2021; Tschida et al., 2019). Here we extend those observations by showing its role as an important hub for the coordination of anxiety-related vocalization.

The intraneuronal accumulation of manganese is biased toward axon terminals (Bedenk et al., 2018). Therefore, we used retrograde tracing to identify brain structures that project to the PAG and may contribute to the increased manganese accumulation observed at the level of the PAG. Those structures included the mPFC, the lateral septum, the preoptic area, the ventromedial hypothalamic nucleus, and the zona incerta. This is in line with previous findings (Beart et al., 1994; Beitz, 1989; Tovote et al., 2016, for review see Silva and McNaughton, 2019). Electrical stimulation of the prelimbic cortex in rats has been shown to trigger vocalizations (Bennett et al., 2019). To prove a functional involvement of the mPFC-dlPAG projection in sonic vocalization in mice, we employed a double-viral chemogenetic approach to selectively inhibit this projection during tail suspension. Although the intervention proved to be capable of modulating behavioral responses as seen by decreased avoidance behavior during the Beetle Mania Task (BMT), it was inefficient in affecting sonic vocalization. Even though this finding suggests that the mPFC-dlPAG projection is not essential for this behavior, technical reasons such as a restricted expression of the chemogenetic receptors might be limiting our conclusion.

Given that mice emit sonic calls in both interactions with conspecifics (wriggling, defeat, Ehret, 1974a; Gourbal et al., 2004) and during circa-strike attacks by predators (Blanchard et al., 1998), the question arises as to their ecological relevance. Mice mostly communicate in the ultrasonic range e.g., during courtship (Nyby et al., 1976; Whitney et al., 1974), in female-female interactions (Maggio and Whitney, 1985; Warren et al., 2020) and in the form of isolation-induced pup calls (Sewell, 1970; Zippelius and Schleidt, 1956), to attract mating partners, social partners or maternal care. Ultrasonic communication gives rodents an advantage in evading predator detection, because many predators are unable to hear ultrasonic sounds,

the sound waves are more directional, and attenuate rapidly compared to sounds in the sonic frequency range (Brudzynski, 2009; Brudzynski and Fletcher, 2010). So, why do mice emit squeaks and squeals that are audible to predators and humans? Sonic vocalization in mice has been described in the context of pain (Ehret, 1974; Scott, 1946), when a non-receptive female is approached by a male mouse (Sewell, 1972), in form of wriggling sounds of pups (Ehret and Bernecker, 1986), or during defense (Blanchard et al., 1998). We have shown that the squeaks emitted when held by the tail or in a defeat situation have a fundamental frequency of 3,800 Hz, which is in line with previous reports (Ehret, 1974; Houseknecht, 1968; Lupanova and Egorova, 2015). Evaluation of the spectral features revealed that some calls contain nonlinear features, such as subharmonics and deterministic chaos (Fitch et al., 2002). These spectral elements have previously been described in calls of high arousal like alarm calls and screams across different species including humans (Arnal et al., 2015; Blumstein et al., 2008; Fitch et al., 2002; Lupanova and Egorova, 2015; Schwartz et al., 2020). Nonlinearities make calls evocative and attract the listener's attention (Arnal et al., 2015). Further, these features were found to prevent habituation to the sound (Blumstein and Récapet, 2009; Karp et al., 2014). In particular, subharmonics present an interesting aspect that allows the animal to lower the pitch, a characteristic which receivers associate with larger body size and aggression of the vocalizing animal (Anikin et al., 2021; Morton, 1977).

To assess the impact of sonic calls on potential predators and conspecifics, we designed playback experiments, in which the animals could control the occurrence of sonic calls or white noise as a control sound by their own behavior. Playback experiments have proved as a powerful method to approximate the function of vocalizations in various species, both in a laboratory setting and in the wild (Asaba et al., 2015; Chabout et al., 2015; Fendt et al., 2018; Musolf and Penn, 2012; Seffer et al., 2014; Seyfarth and Cheney, 2003; Wöhr et al., 2016). Here, playback of sonic calls attracted rats, however, only when combined with a stimulus mouse. The same was the case for both HAB and NAB mice. In absence of a stimulus mouse, sonic calls lose their appetitive nature (NAB) or even turn into a repellent signal (HAB). The neural basis of this remarkable social contextualization remains to be shown in future studies.

In the desperate situation of being trapped or caught by a predator, attraction of a conspecific may distract predators and, thus, increase the likelihood to escape. Although the best hearing frequency of *Mus musculus* is near 16 kHz, foxes and cats perceive best sounds of 4 kHz and 8 kHz, respectively (Heffner and Masterton, 1980; Heffner and Heffner, 1985; Malkemper et al., 2015). Intriguingly, hunters regularly use whistles that imitate distress calls in the range of 3 to 10 kHz to lure foxes or feral cats. Assuming that vocalizations are transmitting information, the sender should choose a frequency that triggers the highest responsiveness in the receiver. Under this premise, it is likely that the emission of 3.8 kHz calls by mice and the hearing range of predators have coevolved. Vocalizations addressing a predator have been observed across species and typically increase in rate with closer proximity of the threat (e.g., also a human experimenter). It is assumed that such calls inform the predator that the prey is prepared for defensive actions and counterattack (Litvin et al., 2007). In addition, the squeaks may startle the predator, offering the prey a chance to escape (Driver and Humphries, 1969; Hogstedt, 1983; Wise et al., 1999). Furthermore, the screams of a struggling prey might attract a second predator expecting an easy meal. The subsequent fight between the two rival predators might offer the prey another chance to flee (Hogstedt, 1983). In support of these hypotheses, playback of avian distress calls has indeed shown to trigger approach and to startle predators (Wise et al., 1999).

Taken together, our study provides insights into sonic mouse vocalization as a means of communication under distress that has so far received little to no attention in neurobiological research. So why do mice squeak? Because they are anxious, they show increased activity in the PAG and to attract both conspecifics and predators, possibly improving their chances of escape.

Limitations of the study

Our study comes with several limitations: First, a brain-wide assessment of phasic changes in neuronal activity during tail suspension would supplement our measures of tonic activity. Second, the causal inference of the circuits underlying sonic vocalization is incomplete. Applying a retrograde tracing approach, we could highlight afferent brain structures that might potentially be functionally involved in controlling sonic vocalization. We could exclude a functional involvement of the mPFC – dlPAG projection. Yet, other structures such as hypothalamic PAG inputs remain to be probed. Besides, identifying potential neuronal subsets within the PAG that might specifically control sonic vocalization as opposed to USV

would help to further characterize these different types of vocalization. These results would further give us the opportunity to functionally investigate sonic vocalization in other mouse lines, e.g., by optogenetic activation of the circuit in NAB or B6N mice to trigger vocalization, thereby proving that sonic vocalization is not only a trait of a mouse line originating from selective breeding. Third, our study would profit from insights of playback experiments with other mouse predators such as cats or foxes. Rats are known to be muricide in the wild; however, laboratory rats became tame or were even selectively bred for ease in handling in the lab environment. This restricts our conclusion on the function of sonic calls for aggressive predators.

STAR★METHODS

Detailed methods are provided in the online version of this paper and include the following:

- KEY RESOURCES TABLE
- RESOURCE AVAILABILITY
  - Lead contact
  - Materials availability
  - Data and code availability
- EXPERIMENTAL MODEL AND SUBJECT DETAILS
- METHOD DETAILS
  - Drugs
  - Stereotaxic injections and implantations
  - Behavioral tests
  - Sound analysis
  - Histology
  - Manganese-enhanced magnetic resonance imaging (MEMRI)
- QUANTIFICATION AND STATISTICAL ANALYSIS

SUPPLEMENTAL INFORMATION

Supplemental information can be found online at https://doi.org/10.1016/j.isci.2022.104657.

AUTHOR CONTRIBUTIONS

Conceptualization, J.R., A.J.G., A.C., and C.T.W.; Formal Analysis, J.R., A.J.G., S.F.K., and M.C.; Investigation, J.R., A.J.G., and D.E.H.; Resources, N.S.C.; Writing, J.R. and C.T.W.; Visualization, J.R. and A.J.G.; Supervision, A.C. and C.T.W.; Funding Acquisition, A.C. and C.T.W.

DECLARATION OF INTEREST

The authors declare no competing interests.

REFERENCES

Adametz, J., and O'Leary, J.L. (1959). Experimental mutism resulting from periaqueductal lesions in cats. Neurology 9, 636. https://doi.org/10.1212/WNL.9.10.636.

Almada, R.C., Genewsky, A.J., Heinz, D.E., Kaplick, P.M., Coimbra, N.C., and Wotjak, C.T. (2018). Stimulation of the nigrotectal pathway at the level of the superior colliculus reduces threat recognition and causes a shift from avoidance to approach behavior. Front. Neural Circuits 12, 36. https://doi.org/10.3389/fncir.2018.00036.

Almeida-Corrêa, S., Czisch, M., and Wotjak, C.T. (2018). In vivo visualization of active polysynaptic circuits with longitudinal manganese-enhanced MRI (MEMRI). Front. Neural Circuits 12, 42. https://doi.org/10.3389/fncir.2018.00042.

Anikin, A., Pisanski, K., Massenet, M., and Reby, D. (2021). Harsh is large: nonlinear vocal phenomena lower voice pitch and exaggerate body size. Proc. R. Soc. B Biol. Sci. 288, 20210872. https://doi.org/10.1098/rspb.2021.0872.

Arnal, L.H., Flinker, A., Kleinschmidt, A., Giraud, A.L., and Poeppel, D. (2015). Human screams occupy a privileged niche in the communication soundscape. Curr. Biol. 25, 2051–2056. https://doi.org/10.1016/j.cub.2015.06.043.

Asaba, A., Kato, M., Koshida, N., and Kikusui, T. (2015). Determining ultrasonic vocalization preferences in mice using a two-choice playback test. J. Vis. Exp. 2–9. https://doi.org/10.3791/53074.

Beart, P.M., Summers, R.J., Stephenson, J.A., and Christie, M.J. (1994). Excitatory amino acid projections to the nucleus of the solitary tract in the rat: a retrograde transport study utilizing d-[3H]aspartate and [3H]GABA. J. Auton. Nerv. Syst. 50, 109–122. https://doi.org/10.1016/0165-1838(94)90128-7.

Bedenk, B.T., Almeida-Corrêa, S., Jurik, A., Dedic, N., Grünecker, B., Genewsky, A.J., Kaltwasser, S.F., Riebe, C.J., Deussing, J.M., Czisch, M., and Wotjak, C.T. (2018). Mn2+ dynamics in manganese-enhanced MRI (MEMRI): cav1.2 channel-mediated uptake and preferential accumulation in projection terminals. Neuroimage 169, 374–382. https://doi.org/10.1016/j.neuroimage.2017.12.054.

Beitz, A.J. (1989). Possible origin of glutamatergic projections to the midbrain periaqueductal gray and deep layer of the superior colliculus of the rat. Brain Res. Bull. 23, 25–35. https://doi.org/10.1016/0361-9230(89)90159-7.

Bennett, P.J.G., Maier, E., and Brecht, M. (2019). Involvement of rat posterior prelimbic and cingulate area 2 in vocalization control. Eur. J. Neurosci. 50, 3164–3180. https://doi.org/10.1111/ejn.14477.

Blanchard, R.J., and Caroline Blanchard, D. (1977). Aggressive behavior in the rat. Behav. Biol. 21, 197–224. https://doi.org/10.1016/S0091-6773(77)90308-X.

Blanchard, R.J., Hebert, M.A., Ferrari, P., Palanza, P., Figueira, R., Blanchard, D.C., and Parmigiani, S. (1998). Defensive behaviors in wild and laboratory (Swiss) mice: the mouse defense test

battery. Physiol. Behav. 65, 201–209. https://doi.org/10.1016/S0031-9384(98)00012-2.

Blumstein, D.T. (2007). The evolution, function, and meaning of marmot alarm communication. In Advances in the Study of Behavior, pp. 371–401. https://doi.org/10.1016/S0065-3454(07)37008-3.

Blumstein, D.T., and Récapet, C. (2009). The sound of arousal: the addition of novel non-linearities increases responsiveness in marmot alarm calls. Ethology 115, 1074–1081. https://doi.org/10.1111/j.1439-0310.2009.01691.x.

Blumstein, D.T., Richardson, D.T., Cooley, L., Winternitz, J., and Daniel, J.C. (2008). The structure, meaning and function of yellow-bellied marmot pup screams. Anim. Behav. 76, 1055–1064. https://doi.org/10.1016/j.anbehav.2008.06.002.

BortA., A., Wöhr, M., Schwarting, R.K.W., and BortA, A. (2006). Rat ultrasonic vocalization in aversively motivated situations and the role of individual differences in anxiety-related behavior. Behav. Brain Res. 166, 271–280. https://doi.org/10.1016/j.bbr.2005.08.009.

Bosch, O.J., Krömer, S.A., and Neumann, I.D. (2006). Prenatal stress: opposite effects on anxiety and hypothalamic expression of vasopressin and corticotropin-releasing hormone in rats selectively bred for high and low anxiety. Eur. J. Neurosci. 23, 541–551. https://doi.org/10.1111/j.1460-9568.2005.04576.x.

Brudzynski, S.M. (2009). Communication of adult rats by ultrasonic vocalization: biological, sociobiological, and neuroscience approaches. ILAR J. 50, 43–50. https://doi.org/10.1093/ilar.50.1.43.

Brudzynski, S.M., and Fletcher, N.H. (2010). Rat ultrasonic vocalization: short-range communication. In Handbook of Mammalian Vocalization. An Integrative Neuroscience Approach, S.M. Brudzynski, ed. (Elsevier B.V.), pp. 69–76. https://doi.org/10.1016/B978-0-12-374593-4.00008-5.

Chabout, J., Sarkar, A., Dunson, D.B., and Jarvis, E.D. (2015). Male mice song syntax depends on socia lcontexts and influences female preferences. Front. Behav. Neurosci. 9, 76. https://doi.org/10.3389/fnbeh.2015.00076.

Chen, J., Markowitz, J.E., Lilascharoen, V., Taylor, S., Sheurpukdi, P., Keller, J.A., Jensen, J.R., Lim, B.K., Datta, S.R., and Stowers, L. (2021). Flexible scaling and persistence of social vocal communication. Nature 593, 108–113. https://doi.org/10.1038/s41586-021-03403-8.

Coburn, C.A. (1912). Singing mice. J. Anim. Behav. 2, 364–366. https://doi.org/10.1037/h0070414.

Dice, L.R. (1932). The songs of mice. J. Mammal. 13, 187. https://doi.org/10.2307/1373992.

Driver, P.M., and Humphries, D.A. (1969). The significance of the high-intensity alarm call in captured passerines. Ibis 111, 243–244. https://doi.org/10.1111/j.1474-919X.1969.tb02531.x.

Ehret, G. (1974). Schallsignale der hausmaus (Mus Musculus). Behaviour 52, 38–56. https://doi.org/10.1163/156853975X00100.

Ehret, G., and Bernecker, C. (1986). Low-frequency sound communication by mouse pups (Mus musculus): wriggling calls release maternal behaviour. Anim. Behav. 34, 821–830. https://doi.org/10.1016/S0003-3472(86)80067-7.

Esposito, A., Demeurisse, G., Alberti, B., and Fabbro, F. (1999). Complete mutism after midbrain periaqueductal gray lesion. Neuroreport 10, 681–685. https://doi.org/10.1097/00001756-199903170-00004.

Fanselow, M.S., and Lester, L.S. (1988). A functional behavioristic approach to aversively motivated behavior: predatory imminence as a determinant of the topography of defensive behavior. In Evolution and Learning, R.C. Bolles and M.D. Beecher, eds. (Lawrence Erlbaum Associates, Inc), pp. 185–212.

Fendt, M., Brosch, M., Wernecke, K.E.A., Willadsen, M., and Wöhr, M. (2018). Predator odour but not TMT induces 22-kHz ultrasonic vocalizations in rats that lead to defensive behaviours in conspecifics upon replay. Sci. Rep. 8, 11041. https://doi.org/10.1038/s41598-018-28927-4.

Fenzl, T., and Schuller, G. (2002). Periaqueductal gray and the region of the paralemniscal area have different functions in the control of vocalization in the neotropical bat, Phyllostomus discolor. Eur. J. Neurosci. 16, 1974–1986. https://doi.org/10.1046/j.1460-9568.2002.02261.x.

Fischer, J., and Hammerschmidt, K. (2011). Ultrasonic vocalizations in mouse models for speech and socio-cognitive disorders: insights into the evolution of vocal communication. Genes Brain Behav 10, 17–27. https://doi.org/10.1111/j.1601-183X.2010.00610.x.

Fish, E.W., Sekinda, M., Ferrari, P.F., Dirks, A., and Miczek, K.A. (2000). Distress vocalizations in maternally separated mouse pups: modulation via 5-HT1(A), 5-HT1(B) and GABA(A) receptors. Psychopharmacology (Berl) 149, 277–285. https://doi.org/10.1007/s002130000370.

Fitch, T. (2006). Production of vocalizations in mammals. In Encyclopedia of Language & Linguistics, K. Brown, ed. (Elsevier), pp. 115–121. https://doi.org/10.1016/b0-08-044854-2/00821-x.

Fitch, W., Neubauer, J., and Herzel, H. (2002). Calls out of chaos: the adaptive significance of nonlinear phenomena in mammalian vocal production. Anim. Behav. 63, 407–418. https://doi.org/10.1006/anbe.2001.1912.

Frank, E., Kessler, M.S., Filiou, M.D., Zhang, Y., Maccarrone, G., Reckow, S., Bunck, M., Heumann, H., Turck, C.W., and Landgraf, R. (2009). Stable Isotope Metabolic Labeling with a Novel N-Enriched Bacteria Diet for Improved Proteomic Analyses of Mouse Models for Psychopathologies 4. https://doi.org/10.1371/journal.pone.0007821.

Frank, E., Salchner, P., Aldag, J.M., Salomé, N., Singewald, N., Landgraf, R., and Wigger, A. (2006). Genetic predisposition to anxiety-related behavior determines coping style,

neuroendocrine responses, and neuronal activation during social defeat. Behav. Neurosci. *120*, 60–71. https://doi.org/10.1037/0735-7044.120.1.60.

Gao, S.C., Wei, Y.C., Wang, S.R., and Xu, X.H. (2019). Medial preoptic area modulates courtship ultrasonic vocalization in adult male mice. Neurosci. Bull. *35*, 697–708. https://doi.org/10.1007/s12264-019-00365-w.

Gourbal, B.E.F., Barthelemy, M., Petit, G., and Gabrion, C. (2004). Spectrographic analysis of the ultrasonic vocalisations of adult male and female BALB/c mice. Naturwissenschaften *91*, 381–385. https://doi.org/10.1007/s00114-004-0543-7.

Gray, J.A., and McNaughton, N. (1996). The neuropsychology of anxiety: reprise. Nebr. Symp. Motiv. *43*, 61–134.

Green, D.B., Shackleton, T.M., Grimsley, J.M.S., Zobay, O., Palmer, A.R., and Wallace, M.N. (2018). Communication calls produced by electrical stimulation of four structures in the Guinea pig brain. PLoS One *13*, e0194091. https://doi.org/10.1371/journal.pone.0194091.

Grünecker, B., Kaltwasser, S.F., Peterse, Y., Sämann, P.G., Schmidt, M.V., Wotjak, C.T., and Czisch, M. (2010). Fractionated manganese injections: effects on MRI contrast enhancement and physiological measures in C57BL/6 mice. NMR Biomed. *23*, 913–921. https://doi.org/10.1002/nbm.1508.

Heffner, H., and Masterton, B. (1980). Hearing in Glires: domestic rabbit, cotton rat, feral house mouse, and kangaroo rat. J. Acoust. Soc. Am. *68*, 1584–1599. https://doi.org/10.1121/1.385213.

Heffner, H.E., and Heffner, R.S. (2007). Hearing ranges of laboratory animals. J. Am. Assoc. Lab. Anim. Sci. *46*, 20–22.

Heffner, R.S., and Heffner, H.E. (1985). Hearing range of the domestic cat. Hear. Res. *19*, 85–88. https://doi.org/10.1016/0378-5955(85)90100-5.

Heinz, D.E., Genewsky, A., and Wotjak, C.T. (2017). Enhanced anandamide signaling reduces flight behavior elicited by an approaching robo-beetle. Neuropharmacology *126*, 233–241. https://doi.org/10.1016/j.neuropharm.2017.09.010.

Hernandez-Miranda, L.R., Ruffault, P.L., Bouvier, J.C., Murray, A.J., Morin-Surun, M.P., Zampieri, N., Cholewa-Waclaw, J.B., Ey, E., Brunet, J.F., Champagnat, J., et al. (2017). Genetic identification of a hindbrain nucleus essential for innate vocalization. Proc. Natl. Acad. Sci. USA *114*, 8095–8100. https://doi.org/10.1073/pnas.1702893114.

Hogstedt, G. (1983). Adaptation unto death: function of fear screams. Am. Nat. *121*, 562–570. https://doi.org/10.1086/284083.

Holstege, G., and Subramanian, H.H. (2016). Two different motor systems are needed to generate human speech. J. Comp. Neurol. *524*, 1558–1577. https://doi.org/10.1002/cne.23898.

Holy, T.E., and Guo, Z. (2005). Ultrasonic songs of male mice. PLoS Biol. *3*, e386. https://doi.org/10.1371/journal.pbio.0030386.

Houseknecht, C.R. (1968). Sonographic analysis of vocalizations of three species of mice. J. Mammal. *49*, 555. https://doi.org/10.2307/1378232.

Jürgens, U. (2009). The neural control of vocalization in mammals: a review. J. Voice *23*, 1–10. https://doi.org/10.1016/j.jvoice.2007.07.005.

Jürgens, U. (1994). The role of the periaqueductal grey in vocal behaviour. Behav. Brain Res. *62*, 107–117. https://doi.org/10.1016/0166-4328(94)90017-5.

Jürgens, U., and von Cramon, D. (1982). On the role of the anterior cingulate cortex in phonation: a case report. Brain Lang. *15*, 234–248. https://doi.org/10.1016/0093-934X(82)90058-X.

Karp, D., Manser, M.B., Wiley, E.M., and Townsend, S.W. (2014). Nonlinearities in meerkat alarm calls prevent receivers from habituating. Ethology *120*, 189–196. https://doi.org/10.1111/eth.12195.

Kelly, J.B., and Masterton, B. (1977). Auditory sensitivity of the albino rat. J. Comp. Physiol. Psychol. *91*, 930–936. https://doi.org/10.1037/h0077356.

Kessler, M.S., Bosch, O.J., Bunck, M., Landgraf, R., and Neumann, I.D. (2011). Maternal care differs in mice bred for high vs. low trait anxiety: impact of brain vasopressin and cross-fostering. Soc. Neurosci. *6*, 156–168. https://doi.org/10.1080/17470919.2010.495567.

Kittelberger, J.M., Land, B.R., and Bass, A.H. (2006). Midbrain periaqueductal gray and vocal patterning in a teleost fish. J. Neurophysiol. *96*, 71–85. https://doi.org/10.1152/jn.00067.2006.

Knutson, B., Burgdorf, J., and Panksepp, J. (1999). Anticipation of play elicits high-frequency ultrasonic vocalizations in young rats. J. Comp. Psychol. *112*, 65–73. https://doi.org/10.1037/0735-7036.112.1.65.

Krömer, S.A., Keßler, M.S., Milfay, D., Birg, I.N., Bunck, M., Czibere, L., Panhuysen, M., Pütz, B., Deussing, J.M., Holsboer, F., et al. (2005). Identification of glyoxalase-I as a protein marker in a mouse model of extremes in trait anxiety. J. Neurosci. *25*, 4375–4384. https://doi.org/10.1523/JNEUROSCI.0115-05.2005.

Kyuhou, S.I., and Gemba, H. (1998). Two vocalization-related subregions in the midbrain periaqueductal gray of the Guinea pig. Neuroreport *9*, 1607–1610. https://doi.org/10.1097/00001756-199805110-00064.

Lahvis, G.P., Alleva, E., and Scattoni, M.L. (2011). Translating mouse vocalizations: prosody and frequency modulation1. Genes Brain Behav. *10*, 4–16. https://doi.org/10.1111/j.1601-183X.2010.00603.x.

Lingle, S., Wyman, M.T., Kotrba, R., Teichroeb, L.J., and Romanow, C.A. (2012). What makes a cry a cry? A review of infant distress vocalizations. Curr. Zool. *58*, 698–726. https://doi.org/10.1093/czoolo/58.5.698.

Litvin, Y., Blanchard, D.C., and Blanchard, R.J. (2007). Rat 22 kHz ultrasonic vocalizations as alarm cries. Behav. Brain Res. *182*, 166–172. https://doi.org/10.1016/j.bbr.2006.11.038.

Lukas, M., and Wöhr, M. (2015). Endogenous vasopressin, innate anxiety, and the emission of pro-social 50-kHz ultrasonic vocalizations during social play behavior in juvenile rats. Psychoneuroendocrinology *56*, 35–44. https://doi.org/10.1016/j.psyneuen.2015.03.005.

Lupanova, A.S., and Egorova, M.A. (2015). Vocalization of sex partners in the house mouse (Mus Musculus). J. Evol. Biochem. Physiol. *51*, 324–331. https://doi.org/10.1134/S0022093015040080.

Madisen, L., Garner, A.R., Shimaoka, D., Chuong, A.S., Klapoetke, N.C., Li, L., van der Bourg, A., Niino, Y., Egolf, L., Monetti, C., et al. (2015). Transgenic mice for intersectional targeting of neural sensors and effectors with high specificity and performance. Neuron *85*, 942–958. https://doi.org/10.1016/j.neuron.2015.02.022.

Maggio, J.C., and Whitney, G. (1985). Ultrasonic vocalizing by adult female mice (Mus musculus). J. Comp. Psychol. *99*, 420–436. https://doi.org/10.1037/0735-7036.99.4.420.

Magoun, H.W., Atlas, D., Ingersoll, E.H., and Ranson, S.W. (1937). Associated facial, vocal and respiratory components of emotional expression: an experimental study. J. Neurol. Neurosurg. Psychiatry *S1–17*, 241–255. https://doi.org/10.1136/jnnp.s1-17.67.241.

Malkemper, E.P., Topinka, V., and Burda, H. (2015). A behavioral audiogram of the red fox (Vulpes vulpes). Hear. Res. *320*, 30–37. https://doi.org/10.1016/j.heares.2014.12.001.

Malkesman, O., Scattoni, M.L., Paredes, D., Tragon, T., Pearson, B., Shaltiel, G., Chen, G., Crawley, J.N., and Manji, H.K. (2009). The female urine sniffing test : a novel approach for assessing reward-seeking behavior in rodents. BPS *67*, 864–871. https://doi.org/10.1016/j.biopsych.2009.10.018.

Michael, V., Goffinet, J., Pearson, J., Wang, F., Tschida, K., and Mooney, R. (2020). Circuit and synaptic organization of forebrain-to-midbrain pathways that promote and suppress vocalization. Elife *9*, e63493. https://doi.org/10.7554/ELIFE.63493.

Morton, E.S. (1977). On the occurrence and significance of motivation-structural rules in some bird and mammal sounds. Am. Nat. *111*, 855–869. https://doi.org/10.1086/283219.

Musolf, K., and Penn, D.J. (2012). Ultrasonic vocalizations in house mice: a cryptic mode of acoustic communication. Evol. House Mouse, 253–277. https://doi.org/10.1017/CBO9781139044547.012.

Nyby, J., Dizinno, G.A., and Whitney, G. (1976). Social status and ultrasonic vocalizations of male mice. Behav. Biol. *18*, 285–289. https://doi.org/10.1016/S0091-6773(76)92198-2.

O'Boyle, M. (1974). Rats and mice together: the predatory nature of the rat's mouse-killing response. Psychol. Bull. *81*, 261–269. https://doi.org/10.1037/h0036175.

Perusini, J.N., and Fanselow, M.S. (2015). Neurobehavioral perspectives on the distinction between fear and anxiety. Learn. Mem. *22*, 417–425. https://doi.org/10.1101/lm.039180.115.

Portfors, C.V. (2007). Types and functions of ultrasonic vocalizations in laboratory rats and mice. J. Am. Assoc. Lab. Anim. Sci. 46, 28–34.

Sangiamo, D.T., Warren, M.R., and Neunuebel, J.P. (2020). Ultrasonic signals associated with different types of social behavior of mice. Nat. Neurosci. 23, 411–422. https://doi.org/10.1038/s41593-020-0584-z.

Scattoni, M.L., Crawley, J., and Ricceri, L. (2009). Ultrasonic vocalizations: a tool for behavioural phenotyping of mouse models of neurodevelopmental disorders. Neurosci. Biobehav. Rev. 33, 508–515. https://doi.org/10.1016/j.neubiorev.2008.08.003.

Scattoni, M.L., Ricceri, L., and Crawley, J.N. (2011). Unusual repertoire of vocalizations in adult BTBR T+tf/J mice during three types of social encounters. Genes Brain Behav. 10, 44–56. https://doi.org/10.1111/j.1601-183X.2010.00623.x.

Scearce-Levie, K., Roberson, E.D., Gerstein, H., Cholfin, J.A., Mandiyan, V.S., Shah, N.M., Rubenstein, J.L.R., and Mucke, L. (2008). Abnormal social behaviors in mice lacking Fgf17. Brain Behav. 7, 344–354. https://doi.org/10.1111/j.1601-183X.2007.00357.x.

Schwartz, J.W., Engelberg, J.W.M., and Gouzoules, H. (2020). Was that a scream ? listener agreement and major distinguishing acoustic features. J. Nonverbal. Behav. 44, 233–252. https://doi.org/10.1007/s10919-019-00325-y.

Scott, J.P. (1946). Incomplete adjustment caused by frustration of untrained fighting mice. J. Comp. Psychol. 39, 379–390. https://doi.org/10.1037/h0061897.

Seffer, D., Schwarting, R.K.W., and Wöhr, M. (2014). Pro-social ultrasonic communication in rats: insights from playback studies. J. Neurosci. Methods 234, 73–81. https://doi.org/10.1016/j.jneumeth.2014.01.023.

Sewell, G.D. (1970). Ultrasonic communication in rodents. Nature 227, 410. https://doi.org/10.1038/227410a0.

Sewell, G.D.S. née (1972). Ultrasound and mating behaviour in rodents with some observations on other behavioural situations. J. Zool. 168, 149–164. https://doi.org/10.1111/j.1469-7998.1972.tb01345.x.

Seyfarth, R.M., and Cheney, D.L. (2003). Meaning and emotion in animal vocalizations. Ann. N. Y. Acad. Sci. 1000, 32–55. https://doi.org/10.1196/annals.1280.004.

Shen, J.-X., Feng, A.S., Xu, Z.-M., Yu, Z.-L., Arch, V.S., Yu, X.-J., and Narins, P.M. (2008). Ultrasonic frogs show hyperacute phonotaxis to female courtship calls. Nature 453, 914–916. https://doi.org/10.1038/nature06719.

Shipley, M.T., Ennis, M., Rizvi, T.A., and Behbehani, M.M. (1991). Topographical specificity of forebrain inputs to the midbrain periaqueductal gray: evidence for discrete longitudinally organized input columns. In The Midbrain Periaqueductal Gray Matter, A. Depaulis and R. Bandler, eds. (Springer US), pp. 417–448. https://doi.org/10.1007/978-1-4615-3302-3_22.

Silva, C., and McNaughton, N. (2019). Are periaqueductal gray and dorsal raphe the foundation of appetitive and aversive control? A comprehensive review. Prog. Neurobiol. 177, 33–72. https://doi.org/10.1016/j.pneurobio.2019.02.001.

Skultety, F.M. (1962). Experimental mutism in dogs. Arch. Neurol. 6, 235–241. https://doi.org/10.1001/archneur.1962.00450210063007.

Sutton, D., Larson, C., and Lindeman, R.C. (1974). Neocortical and limbic lesion effects on primate phonation. Brain Res. 71, 61–75. https://doi.org/10.1016/0006-8993(74)90191-7.

Tovote, P., Esposito, M.S., Botta, P., Chaudun, F., Fadok, J.P., Markovic, M., Wolff, S.B.E., Ramakrishnan, C., Fenno, L., Deisseroth, K., et al. (2016). Midbrain circuits for defensive behaviour. Nature 534, 206–212. https://doi.org/10.1038/nature17996.

Tschida, K., Michael, V., Takatoh, J., Han, B.X., Zhao, S., Sakurai, K., Mooney, R., and Wang, F. (2019). A specialized neural circuit gates social vocalizations in the mouse. Neuron 103, 459–472.e4. https://doi.org/10.1016/j.neuron.2019.05.025.

Warren, M.R., Clein, R.S., Spurrier, M.S., Roth, E.D., and Neunuebel, J.P. (2020). Ultrashort-range, high-frequency communication by female mice shapes social interactions. Sci. Rep. 10, 2637. https://doi.org/10.1038/s41598-020-59418-0.

Wetzel, D.M., Kelley, D.B., and Campbell, B.A. (1980). Central control of ultrasonic vocalizations in neonatal rats: I. Brain stem motor nuclei. J. Comp. Physiol. Psychol. 94, 596–605. https://doi.org/10.1037/h0077699.

Whitney, G., Alpern, M., Dizinno, G., and Horowitz, G. (1974). Female odors evoke ultrasounds from male mice. Anim. Learn. Behav. 2, 13–18. https://doi.org/10.3758/BF03199109.

Wigger, A., Loerscher, P., Weissenbacher, P., Holsboer, F., Landgraf, R., and Wigger, A. (2001). Cross-fostering and cross-breeding of HAB and LAB rats: a genetic rat model of anxiety. Behav. Genet. 31, 371–382. https://doi.org/10.1023/A:1012222402346.

Wise, K., Conover, M., and Knowlton, F. (1999). Response of coyotes to avian distress calls: testing the startle-predator and predator-attraction hypotheses. Behaviour 136, 935–949. https://doi.org/10.1163/156853999501658.

Wöhr, M., and Schwarting, R.K.W. (2013). Affective communication in rodents: ultrasonic vocalizations as a tool for research on emotion and motivation. Cell Tissue Res. 354, 81–97. https://doi.org/10.1007/s00441-013-1607-9.

Wöhr, M., Seffer, D., and Schwarting, R.K.W. (2016). Studying socio-affective communication in rats through playback of ultrasonic vocalizations. Curr. Protoc. Neurosci. 75, 8.35.1–8.35.17. https://doi.org/10.1002/cpns.7.

Yang, M., Farrokhi, C., Vasconcellos, A., Blanchard, R.J., and Blanchard, D.C. (2006). Central infusion of ovine CRF (oCRF) potentiates defensive behaviors in CD-1 mice in the Mouse Defense Test Battery (MDTB). Behav. Brain Res. 171, 1–8. https://doi.org/10.1016/j.bbr.2006.03.013.

Zhang, S.P., Davis, P.J., Bandler, R., and Carrive, P. (1994). Brain stem integration of vocalization: role of the midbrain periaqueductal gray. J. Neurophysiol. 72, 1337–1356. https://doi.org/10.1152/jn.1994.72.3.1337.

Zippelius, H.M., and Schleidt, W.M. (1956). Ultraschall-Laute bei jungen Mäusen. Naturwissenschaften 43, 502. https://doi.org/10.1007/BF00632534.

STAR★METHODS

KEY RESOURCES TABLE

REAGENT or RESOURCE	SOURCE	IDENTIFIER
Antibodies		
Mouse monoclonal anti-EBFP	abcam	Cat# ab32791; RRID: AB_873781
Rabbit polyclonal anti-mCherry	abcam	Cat# ab167453; RRID: AB_2571870
Goat anti-mouse Alexa Fluor® 594	Thermo Fisher Scientific	Cat# A-11032; RRID: AB_2534091
Goat anti-rabbit Alexa Fluor® 488	Thermo Fisher Scientific	Cat# A-11034; RRID:AB_2576217
Bacterial and virus strains		
AAVrg-pmSyn-EBFP-Cre	Madisen et al., 2015	Addgene, 51507
AAV1/2-hSyn-DIO-hM4D-mCherry	Max Planck Institute of Psychiatry	N/A
AAV2-eSyn-EGFP	Vector Biolabs	Cat# VB1107
Chemicals, peptides, and recombinant proteins		
URB597	Sigma-Aldrich	CAS: 546141-08-6
SR141716A	Sigma-Aldrich	CAS: 158681-13-1
Diazepam	Ratiopharm	N/A
Clozapine N-oxide	Tocris	Cat# 4936
Muscimol	Sigma-Aldrich	CAS: 2763-96-4
Muscimol, BODIPY™ MR-X conjugate	Thermo Fisher Scientific	Cat# M23400
Manganese(II) chloride tetrahydrate	Sigma-Aldrich	CAS: 13446-34-9
Critical commercial assays		
M.O.M.® Immunodetection Kit Basic	Vector Laboratories	Cat# BMK-2202
Experimental models: Organisms/strains		
C57BL/6NCrl mice	Charles River Laboratories	CRL: 027; MGI:2683688
BALB/cAnNCrl mice	Charles River Laboratories	CRL: 028; MGI:2683685
DBA/2NCrl	Charles River Laboratories	CRL: 026; MGI:3713843
CD-1 mice	Charles River Laboratories	CRL: 022; MGI:5649524
High-anxiety-related behavior mice	Krömer et al., 2005; Max Planck Institute of Biochemistry, Martinsried	MGI:6488429
Normal-anxiety-related behavior mice	Krömer et al., 2005; Max Planck Institute of Biochemistry, Martinsried	N/A
Long-Evans rats	Charles River Laboratories	CRL: 006
Software and algorithms		
Avisoft RECORDER	Avisoft Bioacoustics	http://www.avisoft.com/recorder/
ANY-maze	Stoelting Co.	https://www.any-maze.com/
EthoVision XT 14	Noldus Information Technology	https://www.noldus.com/ethovision-xt
Raven Pro, Interactive Sound Analysis Software Version 1.5	The Cornell Lab of Ornithology	https://ravensoundsoftware.com/software/raven-pro/
Python 2.7	Python Software Foundation	https://www.python.org/download/releases/2.7/

(Continued on next page)

Continued

REAGENT or RESOURCE	SOURCE	IDENTIFIER
ParaVision	Bruker BioSpin	https://www.bruker.com/de/products-and-solutions/preclinical-imaging/paravision-360.html
Statistical Parametric Mapping	The Wellcome Centre for Human Neuroimaging	https://www.fil.ion.ucl.ac.uk/spm/
GraphPad Prism 9.1	GraphPad Software	https://www.graphpad.com/

RESOURCE AVAILABILITY

Lead contact

Further information and requests for resources and reagents should be directed to and will be fulfilled by the lead contact Dr. Carsten T. Wotjak (carsten.wotjak@boehringer-ingelheim.com).

Materials availability

This study did not generate new unique reagents.

Data and code availability

- All data reported in this paper will be shared by the lead contact upon request.

- All original code is available in this paper's supplemental information.

- Any additional information required to reanalyze the data reported in this paper is available from the lead contact upon request.

EXPERIMENTAL MODEL AND SUBJECT DETAILS

Adult male C57BL/6NCrl (B6N; n = 38, 6 months age), BALB/cAnNCrl (BALB/c; n = 30, 5 months age), and DBA/2NCrl (DBA, n = 12, 4 moths age) mice were purchased from Charles River Laboratories (Sulzfeld, Germany). High-anxiety-related behavior (HAB; male n = 235, 2–9 months age; female n = 36, 2–4 months age), normal-anxiety-related behavior (NAB; male n = 91, 4–7 months age; female n = 8, 4 months age), both originating from a selective breeding approach which started with CD 1 outbred mice (Krömer et al., 2005) and male Crl:CD1 (CD-1; n = 12, 4 months age) mice were bred in the vivarium of the Max Planck Institute of Biochemistry (Martinsried, Germany). After admission to the Max Planck Institute of Psychiatry, mice were permitted a recovery period of at least 10 days before starting with the experiments. Due to changes in the animal facility of the Max Planck Institute of Psychiatry, over time mice had to be housed under different conditions. All animals were group-housed under standard housing conditions (20–22°C room temperature, 50–60% humidity) in either Makrolon type II cages or Green Line IVC mouse cages with food and water *ad libitum*. Mice were kept under SPF conditions which were confirmed by biannual health monitoring using sentinel mice. A 12/12-h normal or inverse light/dark cycle (6 a.m.–6 p.m.) was maintained. For within-strain comparisons, littermates of the same sex were randomly assigned to experimental groups. All mouse experiments were performed according to the European Community Council Directive 2010/63/EEC and approved by the local government of Upper Bavaria (55.2-1-54–2531: 44-09, 188-12, 142-12, 133-06, 55.2–2532: Vet_03-16-08, Vet_02-17-223). All efforts were made to reduce the number of experimental animals used and to minimize any suffering.

Adult male Long-Evans rats (Crl:LE, n = 13, 2 months age) were group-housed under standard housing conditions (22°C room temperature, 40% humidity) at the Institute of Biomedical Sciences of the University of São Paulo, São Paulo, Brazil. Rats were kept in open cages with food and water *ad libitum* and maintained in a 12/12-h normal light/dark cycle (lights on at 6 a.m.). All experimental procedures with rats had been approved by the Committee on the Care and Use of Laboratory Animals of the Institute of Biomedical Sciences, University of São Paulo, Brazil (Protocol No. 085/2012).

METHOD DETAILS

Drugs

URB597 (0.3 or 1 mg/kg; Sigma-Aldrich, St. Louis, MO, USA) and SR141716A (3 mg/kg; Sigma-Aldrich) were dissolved in 15% dimethyl sulfoxide, 4.25% polyethylene glycol, 4.25% Tween 80, and 76.5% saline.

Diazepam (DZP, 1 mg/kg; Ratiopharm, Ulm, Germany) was dissolved in physiological saline. The drugs were injected intraperitoneally (*i.p.* at 10 mL/kg) 1 h prior to the behavioral paradigm. To activate DREADDs, clozapine *N*-oxide (CNO; Tocris, Bristol, Great Britain) dissolved in physiological saline was injected *i.p.* at 10 mg/kg and 10 mL/kg 45 min before exposure to the behavioral test.

Muscimol (MUSC; Sigma-Aldrich) and fluorescently-labeled MUSC (fMUSCL; BODIPY™ TMR-X conj., Thermo Fisher Scientific, Waltham, MA, USA) were dissolved in freshly-prepared artificial cerebrospinal fluid (aCSF) and injected locally via guide cannulas 45 min prior to behavioral testing at 0.1 ng/nL. Vocalization experiments were conducted using fMUSC in a crossover design whereby half of the animals received fMUSC and the other half vehicle (aCSF). On the next day, the treatment was switched. For the elevated plus maze (EPM) experiment mice received MUSC or vehicle.

Stereotaxic injections and implantations

For all stereotaxic surgeries, mice were deeply anesthetized and then maintained at surgical tolerance with isoflurane (CP-Pharma, Burgdorf, Germany) in oxygen-enriched air. Pre-surgical analgesia was provided via subcutaneous (*s.c.*) injections of 5 mg/kg meloxicam (Metacam, Boehringer Ingelheim, Ingelheim am Rhein, Germany) and 200 mg/kg metamizole (Vetalgin®, MSD Animal Health). Post-surgery, the animals were checked on daily and treated with 5 mg/kg meloxicam *s.c.* if needed for 3 days. Stereotaxic injections were delivered using a glass syringe connected to a micropump system (UMP3 and Micro4, World Precision Instruments, Sarasota, FL, USA). All coordinates were validated and adapted to the CD-1 strain. For targeting the dlPAG the following coordinates were used: AP -4.38 mm, ML ±0.3 mm, DV -2.20 mm. Fluoro-Gold (FG, 4%, 350 nL; Fluorochrome, Denver, CO, USA) was injected unilaterally while all adeno-associated virus (AAV) injections were performed bilaterally. For double-viral targeting, 300 μL AAVrg-pmSyn-EBFP-Cre (Madisen et al., 2015, #51507, Addgene, Watertown, MA, USA) were injected at a titer of 7.6 × 10⁹ gc/μL into the dlPAG. One week later, AAV1/2-hSyn-DIO-hM4D-mCherry (titer: 5 × 10⁹ gc/μL) or AAV2-eSyn-EGFP (titer: 7.6 × 10⁹ gc/μL; #VB1107, Vector Biolabs, Malvern, PA, USA) were injected into the medial prefrontal cortex (mPFC, AP +1.20 mm, ML ±0.3 mm) at two dorsoventral positions (DV 1.80 and 2.40 mm), 250 nL respectively. Animals were allowed 3 weeks of recovery before subjected to behavioral testing.

For local MUSC injections, guide cannulas (L3 mm, 26 gauge; World Precision Instruments) were implanted bilaterally at AP -4.25 mm, ML ±1.02 mm, DV -1.55 mm with an angle of ±25°. With an injection needle of 4 mm length, the target injection site was at AP -4.25 mm, ML ±0.6 mm, DV -2.45 mm. The cannulas were fixed to the skull with skull screws positioned above the hippocampus and dental cement (Paladur®; Kulzer, Hanau, Germany). To prevent clogging, dummy injection needles (L3.5 mm) with a dust cap were inserted into the guide cannulas. After allowing at least 2 weeks of recovery, the animals were lightly anesthetized (2–2.5% of isoflurane) for the injection of 100 nL of MUSC or vehicle at 100 nL/min bilaterally via the guide cannulas.

Behavioral tests

All behavioral experiments and their analyses were performed by experimenters blinded to treatment groups and strain, if applicable.

Tail suspension test (TST) and sound recording

Mice were attached to a vertical metal rod with lightly adhesive tape at a height of about 45 cm above ground. Light conditions were at 80–100 lx. A CM16/CMPA ultrasound microphone (Avisoft Bioacoustics, Glienicke, Germany) connected to an UltraSoundGate 116 (Avisoft Bioacoustics) was placed in 25 cm distance from the mouse. Sound was recorded using Avisoft RECORDER (Version 2.9) and mice were video-taped using ANY-maze tracking software (Stoelting Co., Dublin, Ireland) to allow scoring of mobility behavior by a trained observer. The test lasted for 2.5 or 5 min. Animals that climbed up their tail during the test were excluded from the analysis.

Hot Plate Test

To test for thermal pain sensitivity, mice were placed on a warm metal surface (53 ± 0.1°C) surrounded by a cubic Plexiglas wall (Ugo Basile, Gemonio, Italy). The latency to hind paw flicks or licks was measured with a stopwatch. If no reaction was observed, the test was stopped after 30 s.

Social defeat

Male HAB or B6N mice were placed into the open top home cages of male single-housed CD-1 resident mice. Vocalization was recorded using a CM16/CMPA ultrasound microphone. The test was terminated, and the intruder mouse removed, once approximately 15 calls were recorded, the attacks accumulated to avoid wounding or after 10 min of testing.

Social interaction with female mice

Male mice were placed into a square cage with transparent Plexiglas walls and an open top (L40 × W40 × H35 cm) without bedding (to avoid background noise). After a habituation period of 5 min, a female mouse of the same strain was also put in the cage and could freely interact for 10 min. To record ultrasonic vocalization, a CM16/CMPA ultrasound microphone was positioned approximately 25 cm above ground hanging through the open top of the cage. The session was videotaped and the time the male mouse spent sniffing on the female mouse (anogenital and facial sniffing) was scored. The cage was cleaned with soap and water in between each trial.

Elevated plus maze (EPM)

The maze was an elevated (32 cm above ground) plus-shaped platform consisting of two opposite arms enclosed by opaque Plexiglas walls (L27 × W5 x H14 cm) and two opposite arms without walls (L30 × W5 cm, surrounded by a small rim of 0.5 cm height), connected by a central zone (L5 x W5 cm). Mice were placed in the end of one of the closed arms facing the wall. They were allowed to freely explore the maze for 15 min. The experiment was video-recorded, and the time spent in the closed arms was determined. The maze was cleaned with soap and water after each trial.

Beetle Mania Task (BMT)

To test for defensive reactions, the BMT was performed as described previously (Almada et al., 2018; Heinz et al., 2017). In brief: Mice were inserted at one end of a rectangular arena (L100 × W15 × H37 cm) made of gray polyethylene. After a 5-min habitation phase, an erratically moving robo-beetle (Hexbug Nano, Innovation First Labs Inc., Greenville, TX, USA; L4.5 × W1.5 × H1.8 cm) was inserted far most distant from the mouse. During the 10-min test period, avoidance behavior upon contact with the robo-beetle (whereby the mouse withdrew from the robo-beetle with accelerated speed) was scored. The maze was cleaned with soap and water after each trial.

Playback experiments

Using Audacity® open-source software, the stimulus squeak sound was created based on the recording from one male HAB mouse during a TST. The recording contained various sonic calls with the typical characteristics that we had observed in TST-triggered vocalization (for spectrogram see also Figure S5). In order to avoid silent breaks during the playback, the period between two calls was shortened to a maximum of 875 ms which is comparable to that of a naturally occurring train of calls. In this manner, a sequence of 43 different calls (median call duration: 78 ms, with a range of 23–247 ms) with a total length of 21 s was created (see supplemental audio file). During playback, this sequence was seamlessly repeated if needed. A time- and amplitude-matched white noise sound was created as a control stimulus. The sounds were played back at 60–65 dB (i.e., >10 dB above background noise). Sound intensity was measured with a sound level meter (RadioShack, model number 33–2055).

The playback (PB) experiment with mice was performed in a Y-shaped grey polyethylene maze (arm dimensions: W9.5 L30 × H10 cm). Two of the arms were equipped with speakers over each end, the start arm was not. Each rear end of the arms was segregated by a fence. The test animal was placed into the start arm and was automatically tracked using EthoVision XT 14 (Noldus Information Technology, Wageningen, the Netherlands). During the first stage of the test, the baseline (BL) stage, the animal could freely explore the maze without sound presentation for 3 min. In the second stage (PB, 3 min), the squeak sound was automatically presented whenever the animal entered the left arm and continued playing until the animal left the arm. In the same manner, the control sound was played whenever the animal was positioned in the right arm of the maze. No sound was presented in the start arm. In the last stage (PB + S, 3 min), male B6N stimulus mice were constrained to the rear end of the two playback arms, allowing visual, auditory, and olfactory but no physical contact with the test animal. The sounds were presented in the same manner as in the PB stage. The maze was cleaned with soap and water after each trial.

The setup for rats consisted of two transparent Plexiglas boxes (L25 × W25 × H25 cm) connected by a corridor of 100 cm length (W12.5 × H26 cm). The speakers were installed above the two boxes. Transparent plastic containers with holes were fixed in the rear ends of the boxes for stimulus mice. Rats were habituated to the setup on 3 consecutive days, allowing 10 min of free exploration without sound presentation. The playback experiment was performed on the fourth day analogous to the mouse playback experiment. A 3-min BL stage without sound presentation was followed by a 4-min PB stage. The squeaks were played whenever the rat entered the left box and the control sound was presented when it was positioned in the right box. No sound was presented when the rat was in the corridor. During the PB + S stage (4 min), male B6N mice were placed into the containers and the sounds were played back in same manner as in the PB stage. The setup was cleaned with 70% ethanol after each trial.

For both experiments, the time spent in each zone was determined. The Squeak Zone Score was calculated as *time in squeak zone/(time in squeak zone + time in white noise zone)*.

Sound analysis

The number of calls and the call duration were analyzed manually in Raven Pro (Interactive Sound Analysis Software Version 1.5; The Cornell Lab of Ornithology, Ithaca, NY, USA). For analysis of the fundamental frequency of sonic calls, a custom-written Python 2.7 script was used (see Data S1 and S2).

Histology

To verify injection and implantation sites, sections of either freshly frozen or perfused brains were analyzed. For both cases mice were overdosed with isoflurane. To obtain fresh tissue, the brain was dissected from the skull and shortly placed into ice-cold methylbutane. Brains were then stored at −80°C until sectioned using a cryostat. 20 μm sections were mounted directly onto microscopy slides (SuperFrost Plus™, Thermo Fisher Scientific) and stored at −20°C. Transcardial perfusion was performed after respiratory arrest had been confirmed. Cold phosphate buffered saline (PBS) was supplied followed by 4% paraformaldehyde (PFA) in PBS. The brain was dissected from the skull, incubated at 4°C in 4% PFA overnight and subsequently transferred into 30% sucrose in PBS solution. Perfused brains were vibratome-sectioned at 30 μm slice thickness. The slices were stored in cryoprotectant solution at −20°C.

Mice that had received fMUSC injections were perfused 1–3 days after injection. To visualize FG labeling, mice were perfused 1 week after surgery. Brains were freshly frozen from animals of the double-viral experiment 5 weeks after the first viral injection.

To visualize the infection of the tissue with AAVrg-pmSyn-Cre-EBFP and AAV1/2-hSyn-DIO-hM4D-mCherry, their fluorophores were enhanced via immunohistochemistry. The microscope slides were thawed and dried and the sections were fixed with 4% PFA for 30 min. After washing three times with PBS, they were incubated for 1 h in Mouse IgG Blocking Reagent of the M.O.M.® Immunodetection Kit Basic (Vector Laboratories, Burlingame, California, USA). Subsequently, they were washed twice for 2 min in PBS and then incubated for 15 min in M.O.M. Diluent. The primary antibody solution containing the two primary antibodies, M.O.M. Diluent and 0.1% Triton X-100 was applied for overnight incubation. After washing twice in PBS for 4 min, the slices were incubated for 2 h in the secondary antibodies diluted in 1.5% normal goat serum, 0.1% Triton X-100 and PBS. After the final washing steps (three times, for 5 min in PBS), the slides were dried, mounted with mounting medium (DAPI Fluoromount-G®, SouthernBiotech, Birmingham, AL, USA) and covered with a glass slide. The primary and secondary antibodies used were mouse anti-EBFP (1:50, ab32791; Abcam, Cambridge, Great Britain) and anti-mCherry (1:250, ab167453; Abcam), Alexa Fluor® 594 goat anti-mouse (1:250, A-11032; Thermo Fisher Scientific), Alexa Fluor® 488 goat anti-rabbit (1:250, A-11034; Thermo Fisher Scientific).

Immunofluorescence imaging was done using a Axioplan 2 Imaging fluorescence microscope (Zeiss, Oberkochen, Germany).

Manganese-enhanced magnetic resonance imaging (MEMRI)

For detailed description of the procedure and analysis, see Grünecker et al. (2010) (Grünecker et al., 2010). Naïve cohorts of male HAB and NAB mice received *i.p.* injections of 30 mg/kg manganese ($MnCl_2 \cdot 4H_2O$, Sigma-Aldrich) in saline for eight consecutive days. 24 h after the last injection, the MRI experiments were performed in a 7T MRI scanner (Avance Biospec 70/30, Bruker BioSpin, Ettlingen, Germany). The animals

were anesthetized with isoflurane (1.5–1.7% in oxygenated air) and body temperature was constantly monitored and kept at 36–37°C throughout the procedure using a water flow heating pad (Haake S 5P, Thermo Fisher Scientific, Waltham, United States). Data were acquired using a volume resonator for excitation and a saddle shaped surface coil for signal acquisition. T1-weighted images were acquired using a 3D gradient echo pulse sequence (repetition time TE = 50 ms, echo time TE = 3.2 ms) with 10 averages. A matrix of 128 × 128×128 at a field of view of 16 × 16 × 18 mm³ yielding a final resolution of $125 \times 125 \times 140.6 \mu m^3$ was used. Additionally, 3D T2-weighted images were acquired using a rapid acquisition relaxation enhanced (RARE) pulse sequence (TR = 1 s, TE = 10 ms). The same spatial resolution as for T1-weigthed images was acquired, imaging two averages. The reconstructed images (Paravision, Bruker BioSpin, Ettlingen, Germany) were further analyzed using the statistical parametric mapping package SPM5 (using the spmmouse toolbox) and SPM8 (using the segment option for bias correction; www.fil. ion.ucl.ac.uk/spm/). The acquired images of all animals were segmented, exploiting mouse specific tissue probability maps, to obtain bias corrected images. Subsequently, the images were spatially normalized in several steps: 1. Normalization of all images (including brain and extracranial tissue) to a representative single animal image and calculation of the mean normalized image. 2. Creation of a brain mask on the mean normalized image. Brain extraction in native space using the back-transformed mean brain mask. 3. Normalization of the brain extracted images to the group template. Finally, images were smoothed using a Gaussian kernel of eight times the image resolution. Differential manganese accumulation was revealed by pairwise voxel-based comparison between HAB vs. NAB (two sample t-test, corrected for the global signal intensity, masked with a brain mask excluding ventricles, collection threshold at uncorrected p < 0.0001, cluster extent >50; all resulting clusters are significant at $p_{cluster,FEW} < 0.05$).

QUANTIFICATION AND STATISTICAL ANALYSIS

Data are presented as mean values ± standard error (SEM), if appropriate. Statistical details such as the number of animals used can be found in the respective figures and/or figure legends. For normal distribution, paired and unpaired t tests and one-way analysis of variance (ANOVA) followed by Tukey's post-hoc test were performed. In case of not normally distributed data, we applied non-parametric statistics (Kruskal-Wallis or Mann-Whitney U-tests), and for contingency analyses Chi square test. Statistically significant differences were accepted if $p < 0.05$ (indicated by asterisks for normal distribution analysis, by hash symbols for non-normal distribution analysis and dollar symbols for contingency analysis). Statistical analysis was performed using GraphPad Prism 9.1.